Prediction of Nonlinear Resonance in Superconducting Magnetic Levitation Systems (Effect of Excitation Amplitude on Prediction)

TAIGA MIYAHARA* and TOSHIHIKO SUGIURA**
*School of Integrated Design Engineering, Keio University
3-14-1 Hiyoshi, Kohoku-ku, Yokohama, Kanagawa 223-8522, Japan
**Department of Mechanical Engineering, Keio University
3-14-1 Hiyoshi, Kohoku-ku, Yokohama, Kanagawa 223-8522, Japan
E-mail: sugiura@mech.keio.ac.jp

Abstract
A superconducting magnetic levitation system is susceptible to the sudden onset of large amplitude oscillations due to low damping and nonlinear magnetic forces, leading to transitions from stable to unstable states. Furthermore, the eigenfrequency of the levitated body can change with variations in mass or cooling position, highlighting the critical need for accurate identification of parameter conditions that occur resonance. Numerical calculation based on modeling faces challenges in achieving high prediction accuracy because analytical representations of magnetic forces deviate from actual forces. To address these limitations, recent advancements have introduced a data-driven approach, based on bifurcation theory, for predicting resonance in nonlinear systems. This method does not require system modeling. It enables accurate resonance prediction by analyzing changes in damping and angular frequency values, which are derived from response measurements under perturbation as the system approaches a resonant state. In this study, this data-driven approach was applied to superconducting magnetic levitation systems and specifically extended to auto-parametric resonances, which involve the transfer of vibration energy between degrees of freedom. We investigated how excitation amplitude influenced the prediction accuracy of this methodology through a stability analysis of the solutions of the equations of motion, utilizing the method of multiple scales. As a result, we confirmed that increasing the excitation amplitude accelerates the decrease in the frequency component of the perturbation as the excitation frequency approaches the resonance band. Nevertheless, since the tendency for the frequency component difference of the perturbation to decrease is observed even when the excitation amplitude changes, we theoretically demonstrated that this index remains effective for resonance prediction.

Keywords : Superconducting magnetic levitation, Nonlinear resonance, Auto-parametric resonance, Method of multiple scales, Data-driven approach

1. Introduction

A superconducting magnetic levitation system utilizes the pinning effect of superconducting bulks to magnetically levitate permanent magnets. This contactless system is free from friction and can achieve stable levitation without control. This system has potential for various applications, including high-speed transportation and flywheels. However, due to the low damping inherent in non-contact support, the large resonance amplitudes pose a significant challenge to practical applications (Hull, 2000). Furthermore, the eigenfrequency of the levitated body varies with slight changes in mass or cooling position, making it crucial to accurately identify the parameter conditions that induce resonance. Despite this critical need, achieving highly accurate predictions based on system modeling is challenging since the analytical representation of magnetic forces deviates from actual forces (Sugiura and Uematsu, 2000).

Recently, data-driven methods based on bifurcation theory have emerged for predicting resonance in nonlinear systems, relying on response measurements from perturbation instead of modeling (Shiyang and Epureanu, 2018).

Bifurcation is a qualitative change in the state of a system when the parameters governing the system are changed. Focusing on the response displacement when a perturbation is applied to the system, the tendency of changes in damping and angular frequency values as the system approaches the resonance is used to predict resonance.

In this study, we apply this approach to auto-parametric resonance, a type of nonlinear resonance in superconducting magnetic levitation systems in which vibration energy is transferred between degrees of freedom. We investigate the influence of the excitation amplitude on this prediction by a stability analysis of the solution of the equations of motion based on the method of multiple scales (Nayfeh and Mook, 2004).

2. Analytical model and equations of motion

The analytical model is shown in Fig. 1. A rigid body with permanent magnets at both ends is magnetically levitated by Superconducting bulks after field cooling. The system receives harmonic vibration in the vertical direction from a shaker table. The magnetic force acting on the rigid body is analytically expressed using the frozen mirror image method (Kordyuk, 1998). The coordinate system is defined with the z-axis as the vertical direction and the x-axis as the horizontal direction. The origin is set at the static equilibrium point of the levitated body after field cooling. The nondimensional equations of motion in this analytical model are derived as follows, through Taylor expansion of the magnetic forces from the superconductors up to the third order terms:

$$\ddot{z} + \mu_z \dot{z} + z - \alpha_{zz} z^2 - \alpha_{xx} x^2 + \alpha_{zzz} z^3 + \alpha_{xxz} x^2 z = b\nu^2 \cos \nu t \quad (1)$$

$$\ddot{x} + \mu_x \dot{x} + \omega_x^2 x - \alpha_{xz} xz - \alpha_{xxx} x^3 + \alpha_{xzz} xz^2 = 0 \quad (2)$$

where μ are damping coefficients, α are coefficients of the Taylor expansion, b is the excitation amplitude, ν is the excitation angular frequency, and ω_x is the nondimensional angular eigenfrequency of the rigid body in the x-direction. Equations (1) and (2) show that the motions in the x and z directions are coupled through nonlinear terms. Therefore, even though the rigid body is forced to vibrate in the z-direction, it can resonate in the x-direction. This phenomenon is known as auto-parametric resonance, a type of nonlinear resonance where a stable equilibrium or periodic solution loses its stability and branches into new unstable oscillatory states. This resonance involves the transfer of vibrational energy between different degrees of freedom. The nonlinear characteristics of these equations of motion lead to the occurrence of this resonance only under specific conditions of eigenfrequency and excitation frequency.

The frequency response curves and the neutral curve discussed in this section are obtained through the method of multiple scales, which is presented in the next chapter. Figures 2 and 3 show the frequency response curves of the steady-state amplitudes of displacement in the z-direction and in the x-direction, respectively, with ω_x set to 0.50 (i.e., the ratio of the vertical to horizontal eigenfrequency is 2 to 1). These figures demonstrate that auto-parametric resonance occurs only within a specific range of excitation frequencies and that its onset can be sudden.

In contrast, Fig. 4 shows the neutral curve in a plane with the excitation angular frequency ν and the excitation amplitude b as the two axes. This curve represents the boundary where the semi-trivial solution (the solution with no horizontal oscillation, $x = 0$) transitions from a stable to an unstable state, indicating the threshold for resonance occurrence. From this neutral curve, it can be seen that a larger excitation amplitude b leads to a wider frequency band in which resonance occurs.

3. The method of multiple scales

While exact analytical solutions for Eq. (1) and (2) cannot be obtained, approximate solutions can be derived. The method used for this purpose is the method of multiple scales, a type of perturbation method. The method of multiple sc-

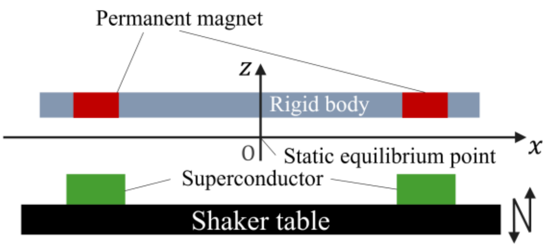

Fig. 1 Analytical model of the system.

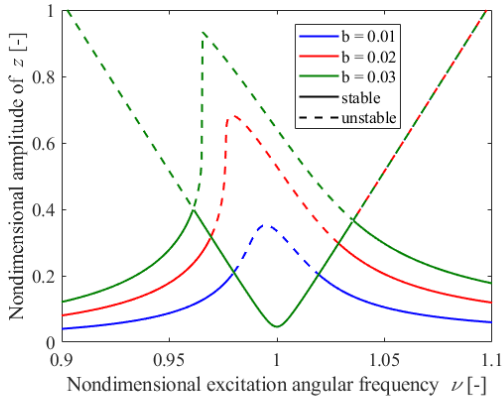

Fig. 2 Frequency response of amplitude of $z(t)$

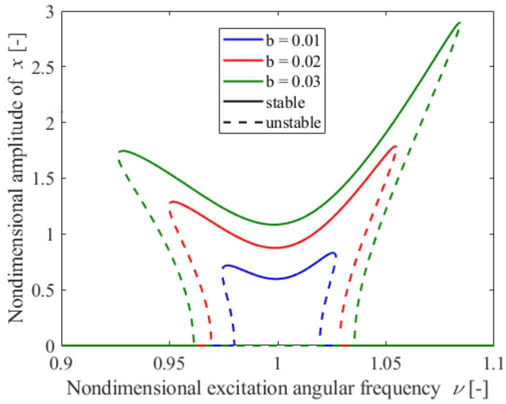

Fig.3 Frequency response of amplitude of x(t)

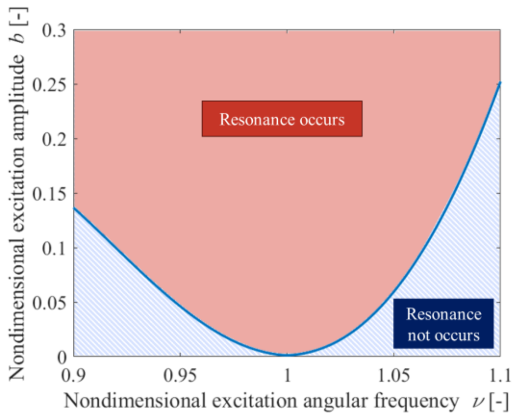

Fig. 4 Neutral curve.

ales is a perturbation technique that introduces multiple time scales to analyze nonlinear oscillatory systems, enabling the derivation of approximate solutions and the examination of their stability. By analyzing the stability of the semi-trivial solution ($x = 0$), we investigate the changes in damping and angular frequency characteristics of the perturbation response displacement. For the displacements z and x, we perform a perturbation expansion as follows:

$$z(t) = \epsilon z_1 + \epsilon^2 z_2 + \epsilon^3 z_3 + \cdots \quad (3)$$

$$x(t) = \epsilon x_1 + \epsilon^2 x_2 + \epsilon^3 x_3 + \cdots \quad (4)$$

Next, multiple time scales t_0, t_1, t_2 and their corresponding differential operators are defined as follows:

$$t = t_0,\ \epsilon t = t_1,\ \epsilon^2 t = t_2$$

$$\frac{d}{dt} = \frac{\partial}{\partial t_0} + \epsilon\frac{\partial}{\partial t_1} + \epsilon^2\frac{\partial}{\partial t_2} + \cdots = D_0 + \epsilon D_1 + \epsilon^2 D_2 + \cdots \quad (5)$$

The dimensionless parameters are ordered as follows:

$$\mu_z = \epsilon^2\widehat{\mu_z}, \mu_x = \epsilon^2\widehat{\mu_x}, \alpha_{xx} = \epsilon\widehat{\alpha_{xx}}, \alpha_{xzz} = \epsilon\widehat{\alpha_{xzz}}, \alpha_{xz} = \epsilon\widehat{\alpha_{xz}}, \alpha_{xxx} = \epsilon^2\widehat{\alpha_{xxx}}, \alpha_{xxz} = \epsilon\widehat{\alpha_{xxz}}, b = \epsilon^2\hat{b} \tag{6}$$

The other parameters are assumed to be of $O(1)$. Substituting Eq. (3) to (6) into Eq. (1) and (2), we derive the balance equations for each order of ϵ:

Order ϵ^1 :

$$D_0^2 z_1 + z_1 = 0 \tag{7}$$

$$D_0^2 x_1 + \omega_x^2 x_1 = 0 \tag{8}$$

Order ϵ^2 :

$$D_0^2 z_2 + z_2 = -2D_0 D_1 z_1 + \alpha_{zz} z_1^2 + \hat{b}\nu^2 \cos \nu t_0 \tag{9}$$

$$D_0^2 x_2 + \omega_x^2 x_2 = -2D_0 D_1 x_1 \tag{10}$$

Order ϵ^3 :

$$D_0^2 z_3 + z_3 = -D_1^2 z_1 - 2D_0 D_2 z_1 - D_0\widehat{\mu_z} z_1 - \alpha_{zzz} z_1^3 - 2D_0 D_1 z_2 + 2\alpha_{zz} z_1 z_2 + \widehat{\alpha_{xx}} x_1^2 \tag{11}$$

$$D_0^2 x_3 + \omega_x^2 x_3 = -D_1^2 x_1 - 2D_0 D_2 x_1 - D_0\widehat{\mu_x} x_1 - 2D_0 D_1 x_2 + \widehat{\alpha_{xz}} x_1 z_1 \tag{12}$$

The general solutions z_1 and x_1 for Eq. (7) and (8) are obtained using complex amplitudes A and B, which are independent of time t_0. Here, c.c. denotes the complex conjugate.

$$z_1 = A(t_1, t_2, \cdots)e^{it_0} + \text{c.c.} \tag{13}$$

$$x_1 = B(t_1, t_2, \cdots)e^{i\omega_x t_0} + \text{c.c.} \tag{14}$$

These are the first-order approximate solutions. Next, Eq. (13) and (14) are substituted into Eq. (9) and (10). In the subsequent equations, NST denotes non-secular terms, which are terms that do not lead to unbounded growth in the solution.

$$D_0^2 z_2 + z_2 = -2iD_1 A e^{it_0} + \frac{\hat{b}\nu^2}{2} e^{i\nu t_0} + \text{NST} + \text{c.c.} \tag{15}$$

$$D_0^2 x_2 + \omega_x^2 x_2 = -2i\omega_x D_1 B e^{i\omega_x t_0} + \text{c.c.} \tag{16}$$

Here, the detuning parameters σ and ρ are defined as follows to investigate the condition of resonance occurrence. σ represents the detuning related to the excitation angular frequency, while ρ represents the detuning of angular eigenfrequency in *z*-direction from twice the angular eigenfrequency in *x*-direction.

$$\sigma = 1 + \sigma = 1 + \epsilon^2\hat{\sigma} \tag{17}$$

$$2\omega_x = 1 + \rho = 1 + \epsilon^2\hat{\rho} \tag{18}$$

The values of secular terms must be suppressed to zero to avoid unbounded solutions in the differential equations. By introducing these detuning parameters, the conditions for eliminating secular terms in Eq. (15) and (16) are obtained:

$$D_1 A = -i\frac{\hat{b}\nu^2}{4} e^{i\hat{\sigma}t_2} \tag{19}$$

$$D_1 B = 0 \tag{20}$$

Consequently, z_2 and x_2 are obtained. Substituting them into Eq. (9) and (10), and by similarly applying the secular term elimination condition, we obtain the following expressions:

$$D_2 A = \widehat{K_{a1}} A + iK_{a2}|\text{A}|^2\text{A} + \widehat{K_{a3}} e^{i\hat{\sigma}t_2} + i\widehat{K_{a4}} B^2 e^{i\hat{\sigma}t_2} \tag{21}$$

$$D_2 B = \widehat{K_{b1}} B + i\widehat{K_{b2}} A\bar{B} e^{-i\hat{\rho}t_2} \tag{22}$$

Here, K are coefficients introduced for simplification. To solve Eq. (21) and (22), complex amplitudes A and B are expressed using real variables A_r, A_i, B_r and B_i, as follows:

$$A(t_2) = (A_r + iA_i)e^{i\hat{\sigma}t_2} \tag{23}$$

$$B(t_2) = (B_r + iB_i)e^{i\frac{\hat{\sigma}-\hat{\rho}}{2}t_2} \tag{24}$$

Substituting Eq. (23) and (24) into Eq. (21) and (22), we derive the identities for the real and imaginary parts. At this stage, the hat notation is removed based on the order evaluation of each parameter.

$$A_r' = K_{a1}A_r + [\sigma - K_{a2}(A_r^2 + A_i^2)]A_i + K_{a3} + K_{a4}B_rB_i \tag{25}$$
$$A_i' = [-\sigma + K_{a2}(A_r^2 + A_i^2)]A_r + K_{a1}A_i - K_{a4}(B_r^2 - B_i^2) \tag{26}$$
$$B_r' = K_{b1}B_r + \frac{\sigma - \rho}{2}B_i + (A_rB_i - A_iB_r)K_{b2} \tag{27}$$
$$B_i' = -\frac{\sigma - \rho}{2}B_r + K_{b1}B_i + (A_rB_r - A_iB_i)K_{b2} \tag{28}$$

Regarding Eq. (25) to (28), in order to consider the time history when a perturbation is applied in the *x*-direction to the semi-trivial solution, B_r and B_i are expressed using their steady-state amplitudes B_{r0} and B_{i0} and small perturbations b_r and b_i as follows:

$$B_r = B_{r0} + b_r \tag{29}$$
$$B_i = B_{i0} + b_i \tag{30}$$

Here, the semi-trivial solution is that the steady amplitude in the *x*-direction is 0; therefore, $B_{r0} = B_{i0} = 0$. Substituting these into Eq. (27) and (28) and expressing them in matrix form. To obtain a tractable analytical solution for the stability analysis, third-order and higher perturbation terms are neglected.

$$\begin{bmatrix} b_r' \\ b_i' \end{bmatrix} = \begin{bmatrix} K_{b1} - A_iK_{b2} & \frac{\sigma - \rho}{2} + A_rK_{b2} \\ -\frac{\sigma - \rho}{2} + A_rK_{b2} & K_{b1} + A_iK_{b2} \end{bmatrix} \begin{bmatrix} b_r \\ b_i \end{bmatrix} \tag{31}$$

From Eq. (31), b_r and b_i can be expressed as follows, utilizing the eigenvalues λ_1 and λ_2 of the matrix and constants C_{r1}, C_{r2}, C_{i1} and C_{i2}:

$$b_r = C_{r1}e^{\lambda_1 t} + C_{r2}e^{\lambda_2 t} \tag{32}$$
$$b_i = C_{i1}e^{\lambda_1 t} + C_{i2}e^{\lambda_2 t} \tag{33}$$

By substituting these into Eq. (24) and subsequently into Eq. (14), the horizontal displacement under small perturbation is obtained as a linear sum of two component waveforms, as follows:

$$x(t) = C_{x1}e^{\mathrm{Re}(\lambda_1)t}\cos\{[\mathrm{Im}(\lambda_1) + \omega_x]t + \phi_1\} + C_{x2}e^{\mathrm{Re}(\lambda_2)t}\cos\{[\mathrm{Im}(\lambda_2) + \omega_x]t + \phi_2\} \tag{34}$$
$$\lambda_1 = -\frac{1}{2}\mu_x + \sqrt{A_z^2\alpha_{xz} - \frac{(\nu - 1)^2}{4}}, \qquad \lambda_2 = -\frac{1}{2}\mu_x - \sqrt{A_z^2\alpha_{xz} - \frac{(\nu - 1)^2}{4}}$$

where A_z is the vibration amplitude of semi-trivial solution of *z*(t). It can be seen that the real part of λ represents the exponential decay constant of the horizontal displacement under small perturbation, and the imaginary part represents the angular frequency.

The exponential decay constant and the angular frequency of the horizontal displacement $x(t)$ under small perturbations for several excitation amplitude conditions are shown in Fig. 5 and 6, respectively. As the excitation angular frequency approaches the resonance band, the difference between the two frequencies decreases (Band I). When this difference reaches zero, damping decreases (Band II), and as the exponent turns positive, resonance occurs (Band III). Due to the low damping characteristics of the superconducting magnetic levitation system, the width of Band II is narrow, meaning that changes in the exponential part are small, making it difficult to predict resonance based on this. On the other hand, in Band I, it is feasible to predict resonance using the difference between the two angular frequencies. Increasing the excitation amplitude widens the resonance bandwidth, and it can be seen that the rate at which the difference between the two frequencies decreases becomes faster as the excitation frequency approaches the resonance band. Nevertheless, in Band I, which lies outside the resonance region on both the lower and higher frequency sides, the frequency difference continues to decrease as the excitation frequency gets closer to the resonance band. This consistent tendency suggests that resonance prediction remains feasible using this approach.

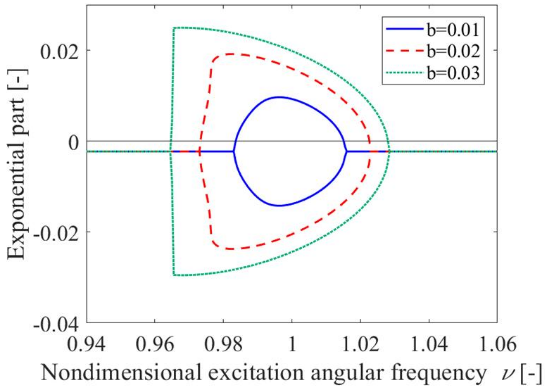

Fig. 5 Dependence of exponential decay constant of horizontal displacement $x(t)$ under small perturbations on vertical excitation frequency ν for different vertical excitation amplitudes b.

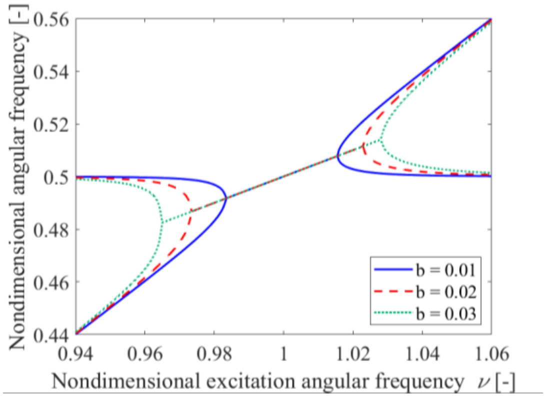

Fig. 6 Dependence of angular frequency of horizontal displacement $x(t)$ under small perturbations on vertical excitation frequency ν for different vertical excitation amplitudes b.

4. Conclusion

This study investigated how changing the excitation amplitude affects the prediction of resonance occurrence in a superconducting magnetic levitation system by using the method of multiple scales. It was shown that increasing the excitation amplitude expands the resonance bandwidth. Moreover, it was confirmed that increasing the excitation amplitude accelerates the decrease in the difference between the two frequencies of the perturbation as the excitation frequency approaches the resonance band. Nevertheless, since the tendency for the frequency difference of the perturbation to decrease is observed even when the excitation amplitude changes, this study theoretically demonstrated that this index remains effective for resonance prediction.

References

Hull, J. R., Topical review: Superconducting bearings, Superconductor Science and Technology, Vol. 13, R1-R15 (2000), pp. 512-520.

Hull, J. R. and Cansiz, A., Vertical and lateral forces between a permanent magnet and a high-temperature superconductor, Journal of Applied Physics, Vol. 86, No. 11 (1999), pp. 6396–6404.

Kordyuk, A. A., Magnetic levitation for hard superconductors, Journal of Applied Physics, Vol.83, No.1 (1998), pp.610-612.

Nayfeh, A. H. and Mook, D. T., Nonlinear oscillations (2004), pp. 164-165, Wiley-VCH.

Shiyang C. and Epureanu, B. I., Forecasting bifurcations of multi-degree-of-freedom nonlinear systems with parametric resonance, Nonlinear dynamics, Vol.93, No.1 (2018), pp.63-78.

Sugiura, T. and Uematsu, Y., Analysis of electromagnetic force and torque in high-tc superconducting levitation based on the advanced mirror image method, Japan Society of Mechanical Engineering Journal C, Vol. 66, No. 644 (2000), pp. 1138-1145 (in Japanese).